



# Evaluation of antibacterial and mechanical features of dental adhesives containing colloidal gold nanoparticles



Sara Dadkan<sup>a</sup>, Mehrdad Khakbiz<sup>a,\*</sup>, Lida Ghazanfari<sup>b</sup>, Meizi Chen<sup>c</sup>, Ki-Bum Lee<sup>c,\*</sup>

<sup>a</sup> Division of Biomedical Engineering, Faculty of New Sciences and Technologies, University of Tehran, North Kargar Ave, PO Box 14395-1561, Tehran, Iran

<sup>b</sup> Center for Nanotechnology in Drug Delivery, University of North Carolina at Chapel Hill, NC, USA

<sup>c</sup> Department of Chemistry and Chemical Biology, Rutgers, The State University of New Jersey, Piscataway, NJ 08854, USA

## ARTICLE INFO

### Article history:

Received 30 November 2021

Revised 8 July 2022

Accepted 9 July 2022

Available online 15 July 2022

### Keywords:

Dental adhesive

Gold nanoparticles

Antibacterial properties

Mechanical properties

Cytotoxicity

## ABSTRACT

In this study, colloidal gold nanoparticles (NPs) with sizes less than 20 nm were added to the dentin adhesive in various concentrations to achieve favorable antibacterial properties. The effect of gold NPs on mechanical, antibacterial, and cytotoxicity features of adhesive was evaluated systematically. It was shown that the addition of gold NPs at the concentration of 5X (i) increased flexural strength of dentin tooth adhesive by 75%, (ii) increased the micro-shear bond strength by 60%, and (iii) increased the tensile diameter strength of adhesive by 65% compared to the based adhesive. Multiscale modeling was used to simulate and calculate stress and strain distribution around the nanoparticles and within the adhesive matrix. Antibacterial properties of adhesives containing gold NPs were examined using disk diffusion and the pour plate methods. The results showed that adhesive with the 5X concentration of gold NPs had a bacterial growth inhibition zone with a diameter of 2 mm in the disk diffusion method which indicates the antibacterial characteristics of adhesive at this concentration. Also, the antibacterial effect of adhesive-containing NPs was observed in the pour plate method and the reduction of bacterial growth is increased by the addition of nanoparticles. The cytotoxicity of NPs is examined in pure form and combination with dental adhesive using the MTT assay. The results showed that pure gold NPs have shown no toxicity for the growth of cells and the incorporation of gold NPs has increased the cell viability in the base adhesive.

© 2022 Elsevier B.V. All rights reserved.

## 1. Introduction

Adhesive dental materials have led to tremendous improvements in dentistry and has paved the way for clinical advances [1,2]. Adhesion is a force that makes two close things stick together or their molecules will be absorbed. Many approaches can be found in the history of replacing the lost structure of the tooth and the whole tooth. Replacing tooth lost structure due to disease or injury is still considered as a large part of general dentistry. Restorative dental materials are the base for replacing the structure of tooth. The essential considerations in replacing lost teeth structure are their form and function [3].

Due to the increasing development of tooth-colored composites in restorative dentistry, these materials are an appropriate choice in dentistry as they maintain the cosmetic appearance as well as improve the mechanical features. The properties and quality of a composite restoration depend on the method of composite connec-

tion and the connector to the tooth in many cases. Different types of enamel or dentin bonding agents are used to attach composites to tooth which have different features according to applied enamel or dentin composite. Since dentin has a different chemical composition compared to enamel and has living and wet tissue, attaching adhesive reagents to dentin is more difficult than attaching those to the enamel. This issue has led to many efforts to improve the features of adhesive agents. Second caries are the most important reason for the replacement and removal of composite resins. Since caries is an infectious complication and a lot of Streptococcus bacteria mutants separated from carries plaques will cause tooth decay, the use of dental adhesives containing antimicrobial properties would be highly beneficial in the prevention of second caries [4]. Fig. 1 compares two teeth structures with and without biofilm caused by bacteria.

Restorative dental materials that are used today are mostly based on resins made of di methacrylate monomers [5]. These resins suffer volumetric shrinkage during polymerization which is caused by the conversion of van der Waals force to covalent bonds in the polymer. This shrinkage causes a gap between

\* Corresponding authors.

E-mail addresses: [khakbiz@ut.ac.ir](mailto:khakbiz@ut.ac.ir) (M. Khakbiz), [kblee@rutgers.edu](mailto:kblee@rutgers.edu) (K.-B. Lee).

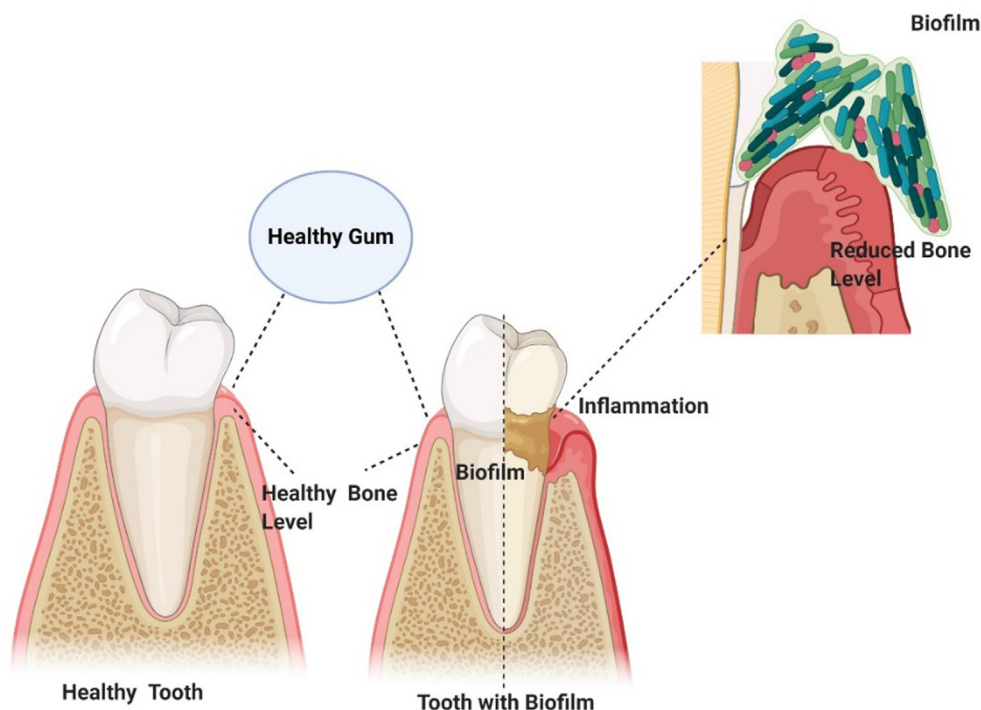


Fig. 1. Comparison of healthy tooth and tooth with biofilm (Created with BioRender).

restorative materials and tooth tissue, creating place for the growth of bacteria in mouth. Antibacterial adhesives can inhibit the remaining bacteria in the tooth cavity and destroy invading bacteria in the cavity and prevent the decay of a re-restored tooth.

Nowadays, the addition of NPs to polymers to improve the mechanical properties is being considered as a principle. The effect of NPs on adhesion can be examined from three hypotheses:

The effects of NPs on wettability: When a particle is added to a liquid or paste since the liquid–liquid interface is replaced with the liquid–solid interface, it seems the wettability angle has increased. The decreased wettability ultimately results in loss of adhesion. On the other hand, adding solid particles to a system increases mechanical interweaving.

The effects of NPs on viscosity: In fact, viscosity is an important parameter in dental adhesives. Lower viscosity leads to further penetration of the adhesive into the tooth bumps and greater connection of tooth and adhesive. It has been found in many cases that adding NPs reduces viscosity [6]. The reason for this phenomenon can be attributed to activation of the roller mechanism of NPs during shear stress. Since NPs used in this system have been a colloidal solution, adding such a solution to the adhesive will ultimately decrease its total viscosity. These two factors are the main reasons for the decrease in viscosity and thus higher adhesion of adhesive.

The effect of gold NPs on hydrophilicity: It has been observed that the higher rate of hydrophilicity of adhesive will result in the higher adhesion of adhesive to the tooth surface. This is due to the wettability of the dentin surface.

Metals have been investigated as antibacterial agents for many centuries [7]. For instance, gold, silver [8,9], copper [10] and zinc [11–13] are among the materials that have been widely used in this regard. Anti-bacterial properties have been reported in the case of silver and gold NPs added to resin materials [14].

Silver compounds are widely known for their antibacterial property. Due to this property, silver-based nanomaterials are investigated in the application of dentistry, including dental restoration [15]. Ag NPs also share the common advantage of nanomaterials with high specific surface area, contributing to the easier

penetration in the bacterial cell membrane. However, even Ag-based nanomaterials present excellent antibacterial performance, it shows toxicity to cells may change dental color in the long term [16]. Zinc oxide nanoparticle is another emerging nanomaterial that shows antibacterial properties. ZnO exhibits high stability under harsh processing compared with other metal-based nanomaterials [17]. Furthermore, ZnO nanoparticles with appropriate design show selective toxicity to certain bacteria with a minimal negative effect on human cells [18], show selective toxicity to certain bacteria with a minimal negative effect on human cells [18]. In addition, some nanoparticles like as layered double hydroxides (LDH) have antibacterial drug loading capabilities [32,33].

It has been confirmed that gold NPs are active in many important commercial reactions as catalyst and have suitable surface chemistry. New applications of nanotechnology using gold are expanding based on these unique features [19,20]. The supercities of gold nanomaterials compared with other metals lie in their unique properties. Properties of gold particles such as neutrality, idea biocompatibility, low bacterial resistance, lack of cytotoxicity, and resistance to surface oxidation, particularly at the nanoscale, can be effective in the improvement of dental adhesives features [17,21]. To be specific, gold nanoparticles is less cytotoxicity than silver. The results show that silver nanoparticles have more antibacterial properties, but the cytotoxicity of the ions released by silver nanoparticles limits their application in medical and biological sciences [22]. In addition, gold nanoparticles are easily modified so that antibacterial properties can be increased by changing their structure or size. Gold nanoparticles have better surface modification properties than other nanoparticles such as silver, so they can be loaded with other drugs to produce stronger antibacterial properties [23]. Gold NPs with very fine grain sizes can easily penetrate the bacteria or destroy bacteria by covering it and preventing nutrients from reaching the bacteria.

However, similar to other nanoparticles, gold nanoparticles have some benefits and restrictions for other applications. For example, the intracellular delivery of biologics by nanoparticle-sensitized photoporation, a new method that combines great

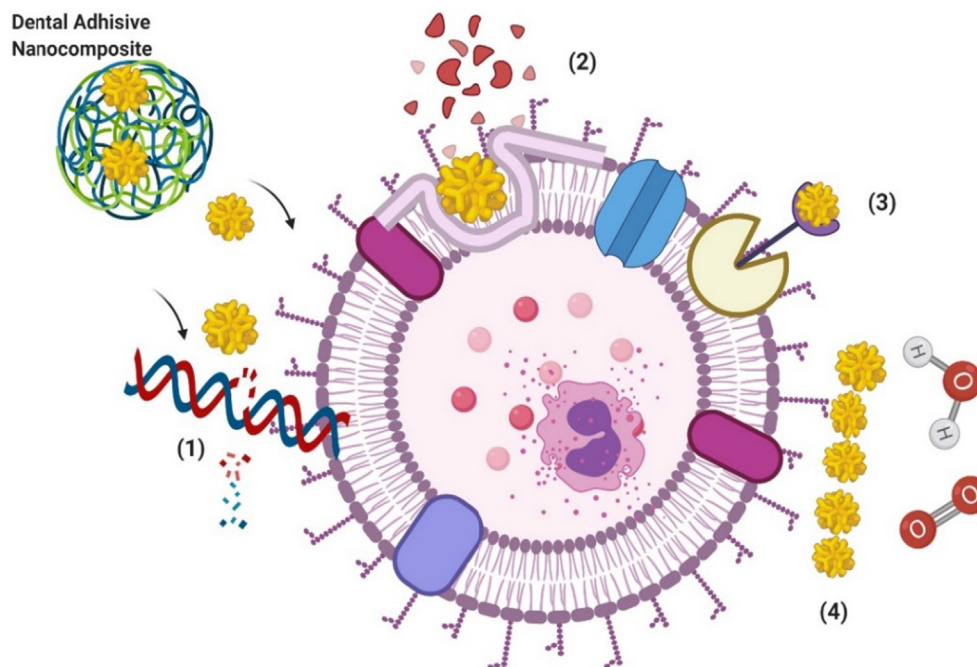


**Fig. 2.** A schematic of the mechanism of killing bacteria by gold NPs: (1) rupturing the bacterial cell membrane, (2) accumulating into the bacteria cell, (3) formation of bands of (SH-) group in the enzymes, (4) destruction of the cytoplasm by NPs (Created with BioRender).

efficiency and throughput with outstanding cell survival, is promising upcoming therapy. It is, however, hindered by safety and regulatory issues since it relies on intimate interaction between nanoparticles and cells. Research has shown [31] that after photoporation with Au NPs, a large proportion of Au stays connected with those cells even after vigorous washing; however, Xiong and et al. [31] demonstrated that the same is true when utilizing iron oxide nanoparticles.

Some major mechanisms of antibacterial NPs are as follows: (i) the NPs penetrate the bacteria and rupture the bacterial cell membrane, (ii) the NPs accumulate around the bacteria and prevent food from getting to bacteria, (iii) the presence of gold NPs near the bacteria leads to the transformation of bacteria and destruction of the cytoplasm of the bacteria, (iv) gold turn into ions which are absorbed by the microbes leading to the formation of bands of the group (SH-) in the enzymes, resulting in the reduction of microbial activity. A schematic of the mechanism of killing bacteria by gold NPs is shown in Fig. 2 [24].

In this study, gold NPs are added to a dentin adhesive system where the objective is to obtain an adhesive with antibacterial feature and improve mechanical property. These properties are verified to prevent the second decay of teeth and increase the lifetime of composite restorations.

## 2. Materials and methods

### 2.1. Materials

The gold nanoparticle sample was purchased from Nano Natural. Gift co (BioGNP) with a purity of more than 97%, and density of 3.18 ng/mL. Bis-GMA. UDMA monomers and Polyurethane de methacrylate monomer were purchased from the Evonik. 2-methyl-2 hydroxyethyl and DL Terry propane methacrylate (TMPTMA), acetone, tryptone, yeast extract, Mueller Hinton broth, and ethanol were purchased from Merck. Ethanol hydroxyethyl (Methacrylate) was purchased from Fluka. Camphorquinone (CQ), HEMA, and N' ·N- Dimethyl amino ethyl methacrylate

(DMAEMA) was purchased from Sigma-Aldrich. The dental composite used in this study was Premise Composite A3 / 5 produced by Kerr America and the 37.5% Phosphoric acid gel of the same company was used as etching dentin factor. Required bacteria including bacteria strains of Staph aureus, Staphylococcus epidermidis, Staphylococcus Saprophyticus, Enterococcus faecalis, and Streptococcus were purchased from Pasteur Institute of Iran. Mueller Hinton agar and agar were purchased from Quelab.

### 2.2. Methodology

#### 2.2.1. Synthesis of adhesive

500 g of dentin adhesive was prepared by the formula outlined in Table 1 and initiator and light activator were not added initially to prevent premature curing. The prepared solution was kept in light-resistant glass in the refrigerator [25].

#### 2.2.2. Extracting water from gold colloidal nanoparticles

To ensure the purity, size, and morphology of gold NPs, XRD, TEM, and spectrophotometry analysis were carried out before mixing them with the adhesive. Gold NPs were centrifuged for 30 min at 14000 rpm to remove all the water from this colloidal solution. Assuming the concentration of initial NPs is X, sediments obtained from the centrifuge process were added to the adhesive at the concentrations of 10X, 5X, and X (Fig. 3 "supporting information").

#### 2.2.3. Preparation of gold NPs containing adhesive

Initially, the monomers and raw materials of the base adhesive were weighed according to formulations mentioned in Table 1 and mixed well in a container resistant to light. The prepared solution was vortexed for 10 s at a low speed. Then, the concentrated gold NPs were added to the base adhesive and the obtained solutions were bath sonicated for 5 min. The light initiator and the light activator were added to the above mixtures in the amount of 5.0 percent. Then, about 2 g of each mixture was isolated and was kept in a dark container in the refrigerator (to carry out a shear strength test). Then, the rest of the mixtures containing different percent-

**Table 1**  
Base adhesive composition.

Operation	Wt%	Material Name
Adhesive monomer	14	Bis-GMA
Adhesive monomer	26	HEMA
Primer	8	TMPTMA
Adhesive monomer	11	UDMA
Solvent adhesives	40	Acetone
Photoinitiator	0.5	Comphorquinon
Active Optical	0.5	DMAEMA

ages of NPs were placed in an oven at ambient temperature for 72 hrs to completely evaporate ethanol. This was done to completely remove the residual solvent and thus to avoid the formation of bubbles in the sample and so to prevent incomplete cooking.

### 2.3. Characterization of samples

#### 2.3.1. Scanning electron microscopy (SEM), X-ray diffraction and UV-Vis spectroscopy

Scanning electron microscope (SEM) HITACHI S4160 was used for investigation of surface fracture of samples and dispersion of NPs in the resin matrix. X-ray diffraction model D8 ADVANCE X-ray diffractometer was used for crystal structures analysis. UV-Vis spectrum Model Lambda 850 was used for particle size measurement.

#### 2.3.2. Flexural strength testing

Flexural strength testing test was performed according to the ISO 4049 standard, using rectangular cube molds with dimensions of  $2 \times 2 \times 2$  mm, as shown in Fig. 4. Fig. 4. b shows the samples prepared after curing the UV device. The three-point bending

was performed by an instrument where the distance of the supports is 20 mm. In this case, a load cell of 200 N and a speed of 0.5 mm/min was applied.

#### 2.3.3. Diametral tensile strength test

Diametral tensile strength test was performed according to ADA 27 standard. For this purpose, cylindrical molds made of stainless steel with a diameter of 6 mm and a height of 3 mm were used. The samples were placed in a universal machine so that they were pressed in a diameter direction. A load cell of 2.5 kN and a speed of 10 mm/min was used for the test (Fig. 5).

#### 2.3.4. Micro shear test

A wire with a diameter of 0.4 mm was looped around the composite cylinder which was attached to tooth surface by sample adhesives. The shear force was applied at a loading speed of 1 mm/min until the specimens were broken and the composite was separated from the tooth (Fig. 6).

#### 2.3.5. Antibacterial test

**2.3.5.1. Disk diffusion method.** A colony of streptococcus mutants, which cultured on medium with Trypton 10%, NaCl 10% Yest extract 5% and agar 15% composition was selected and cultured in Müller-Hington- Broth culture medium (21 g of culture medium was dissolved in 1 L of distilled water and sterilized in an autoclave). The resulting suspension was placed in an incubator at 37° C and its optical density was measured every 30 min with a spectrophotometer until reached the standard opacity. After that, the microbial suspension was ready for culture. The Müller-Hington agar medium, or solid LB, is prepared and poured into a petri dish under sterile conditions in a laminar hood. After it was solidified, the swab was inserted into the falcon tube containing the bacterial suspension and rotated several times. It was then pressed against the wall of the falcon tube above the liquid level

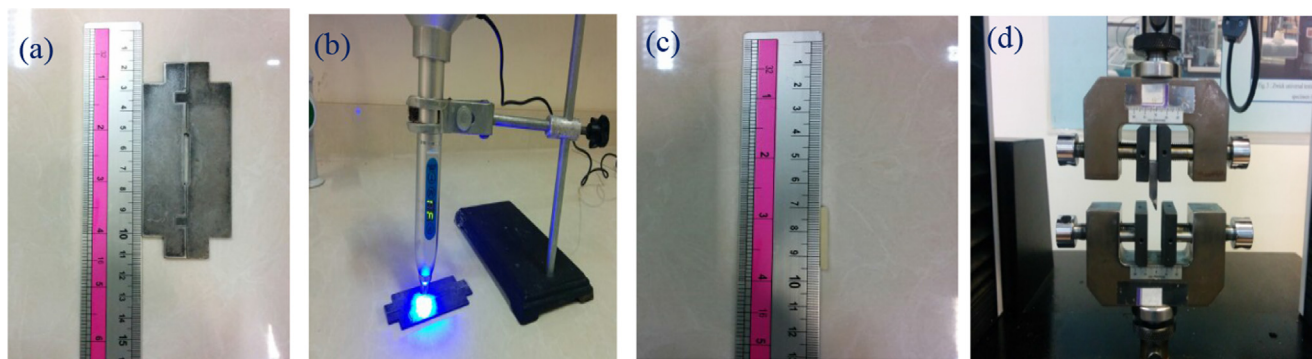


Fig. 4. (a) mold for resin casting, (b) curing with ultraviolet light, (c) cured sample, and (d) mechanical test instrument.



Fig. 5. (a) mold for resin casting, (b) prepared sample, and (c) test instrument.

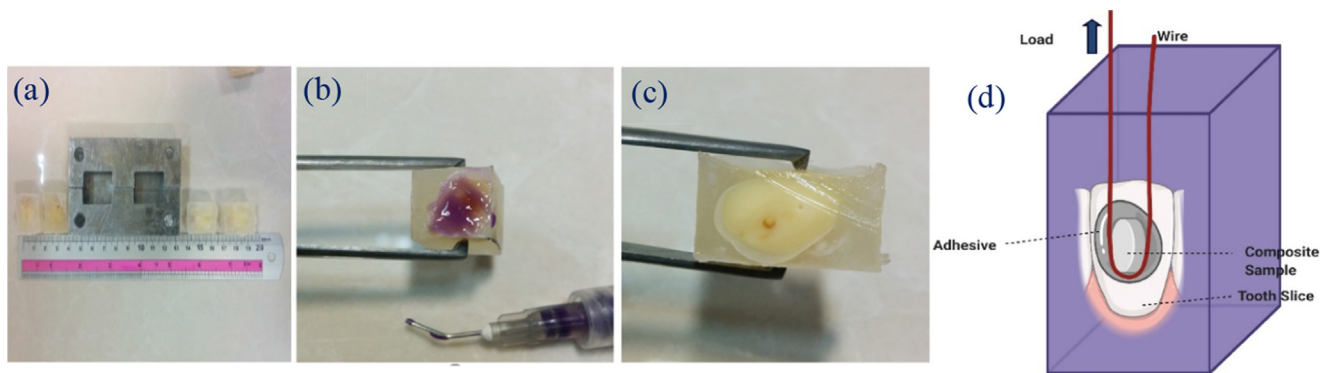


Fig.6. (a) mold for composite, (b) dental adhesive cured on composite, (c) adhere dental to dental composite by adhesive, and (d) micro shear procedure.

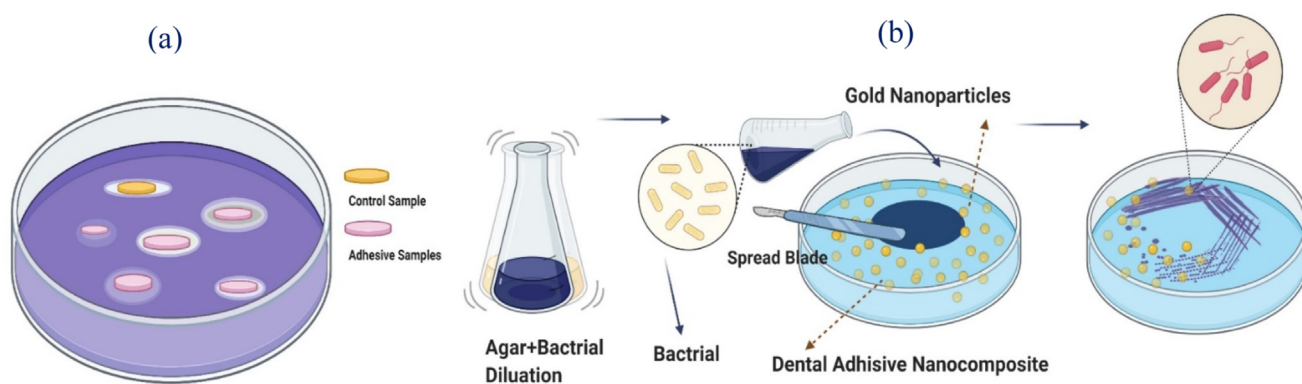


Fig. 7. (a) schematic of disk diffusion method and (b) pour plate method (Created with BioRender).

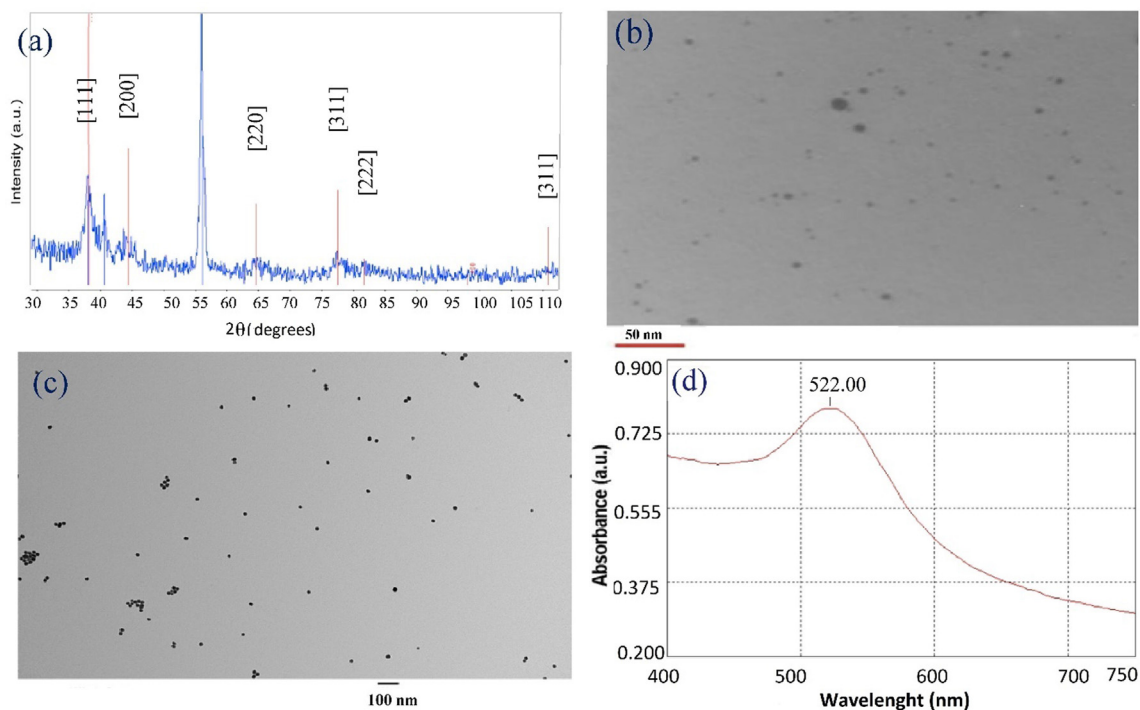


Fig. 8. (a) X-ray diffraction analysis (b) SEM micrograph (c) TEM micrograph and (d) UV-Vis spectrum of gold NPs.

to remove excess liquid. The swab was drawn in parallel lines on the surface of Mülling Hington agar. This was done a total of three times each time with a 60-degree rotation of the petri dish. After inoculation, it was left in a semi-open container for 3 to 5 min to evaporate the excess moisture [29]. NPs in pure form and combination with liquid adhesive at different concentrations were injected on the blank of the disk to impregnate the whole disk, then the disk was evenly placed in a container of Müllerington agar inoculated with bacteria. For each concentration, the disc was inserted in three repetitions, so that the distance between the discs from the center of one disc to the next is not less than 24 mm. Then the petri dish was closed, turned over, and placed in a 37° incubator for 18 hrs. As a positive control, streptomycin antibiotic tablets were dissolved in distilled water and autoclaved to achieve sterile conditions. The resulting liquid was injected on a disk and placed on a petri dish to observe the absence of bacterial growth. Blank disk alone was used as a negative control [30].

**2.3.5.2. Pour plate method.** In the pour plate method, the Müllerington agar culture medium was mixed with gold NPs at different concentrations in a falcon and poured into Petri dishes. After the culture medium was cooled and solidified, some of the prepared microbial suspension was cultured linearly with a swab on Müller Hington. The petri dish was then placed in a 37° incubator for 24 hrs to check for bacterial growth. Fig. 7 shows the schematic of disk diffusion and pour plate method.

### 2.3.6. Cytotoxicity test

L929 fibroblast cell line was purchased as a flask containing newly cultured cells from Pasteur Cell Bank and transferred to a CO<sub>2</sub> incubator with 90% humidity. Different treatment groups were considered including water-soluble NPs at concentrations of 1X, 5X, and 10X, polymer adhesives containing the same number of NPs in both liquid and solid (cured) forms. The control group was a complete culture medium without any additives. The experiment was performed with three replications at 24, 48, and 72 hrs. time intervals. Cell count was performed using trypan blue dye and hemocytometer slide. After preparing a cell suspension with a suitable concentration, they were seeded in the 96-well plate plates at a cell density of 7000 cells per well. After 12 hrs., the cells were treated with adhesives containing different amounts of NPs.

## 3. Results

### 3.1. X-ray diffraction analysis (XRD)

The XRD analysis of freeze-dried gold NPs has been carried out and the results showed that the only known element of the analysis was gold (Au) and the obtained peaks matched the reference peak of gold (00–004–0784) confirming the purity of NPs. The results of XRD in the Xpert application were analyzed based on Bragg's equation ( $n\lambda = 2d \sin\theta$ ), as shown in Fig. 8-a. The peaks shown in Fig. 8-a are matched gold NPs standard peaks. The crystal size of NPs can be calculated based on the peaks and Scherrer equation (Eq. (1)):

$$d = k\lambda/B\cos\theta \quad (1)$$

According to Eq. (1), the mean diameter of gold particles was 18 nm, where  $d$  is the grain size,  $k$  is the Scherrer constant and equal to 0.9,  $\lambda$  is the wavelength of X-ray and equals to 0.154 nm,  $B$  is peak width at half the height and  $2\theta$  is the angle of diffraction.

### 3.2. Spectrophotometry analysis

Given that the color of gold NPs depends on the surface plasmon created by these particles on a nano-scale, the color of particles and the peak of their surface plasmon with a spectrophotometer represent the size and quality of NPs. As shown in the UV-Vis spectrum of gold NPs in Fig. 8-c, the emission peak is at a wavelength of 522 nm and this proves the size of particles is less than 20 nm and that they have spherical morphology.

### 3.3. TEM analysis

In Fig. 8-b, C shows the SEM and TEM image of gold NPs. According to the obtained images, it can be seen that the nanoparticles are almost spherical, and the particle size is less than 20 nm. Of course, the distribution of the particle size range is also wide. Gold nanoparticles of this size may easily penetrate and attach to bacteria. The particle sizes determined by TEM pictures are somewhat larger than those calculated by XRD patterns.

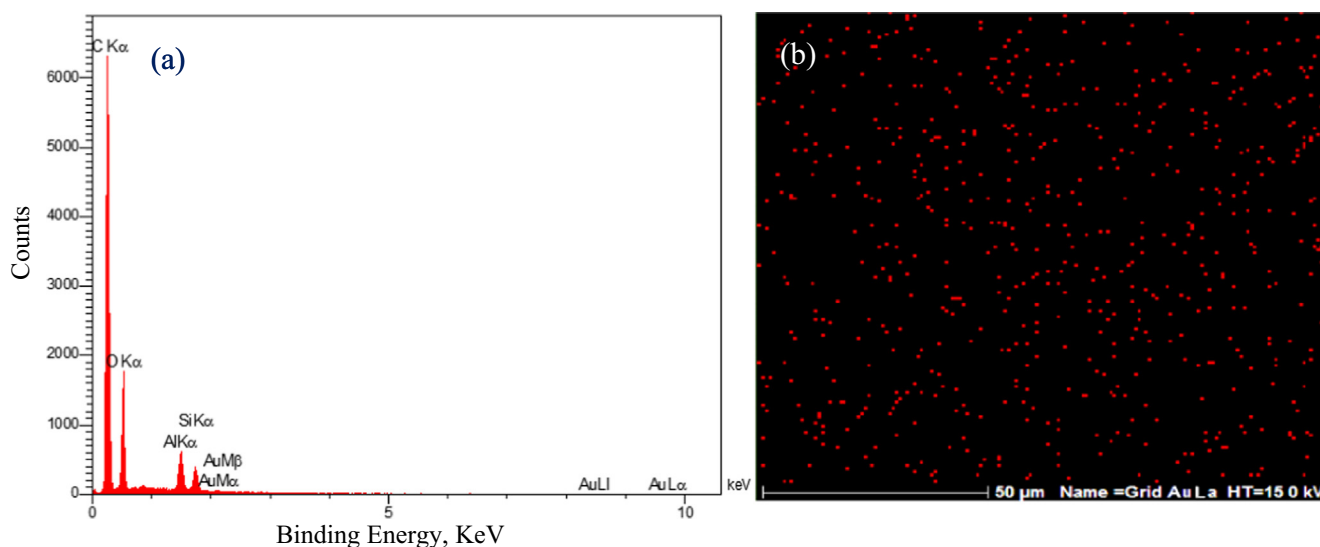


Fig. 9. (a) EDX graph and (b) Map analysis of gold NPs with concentration of 10X in adhesive systems.

### 3.4. EDX analysis of produced adhesive samples

In Fig. 9-a, the peak related to EDX analysis of an adhesive sample with the concentration of 10X shows that the added gold NPs are present in the polymerized adhesive. About 17% weight percent of the gold element is present in the adhesive composition of the solid sample. This shows the incorporation of NPs in the adhesive composition was successful. The 7% excess amount is related to the composition gold coating of the samples for the analysis. Inhomogeneous dispersion of nanoparticles in matrix will result in decreased properties. For instance, cracks can form between clusters of nanoparticles, resulting in a loss in the mechanical characteristics of composites. Fig. 9-b shows elemental map analysis of sample which confirms the homogenous distributions of nanoparticles in matrix. The map analysis in Fig. 9-b shows that gold NPs are well distributed and are stable during the curing process.

### 3.5. Mechanical testing and adhesion strength

The results of the bending test have been shown in Fig. 10-a in form of a stress-strain diagram. The flexural strength has been obtained using these diagrams. This graph demonstrates that nanocomposite adhesives exhibit a combination of elastic and plastic properties and are not entirely brittle. However, samples

with 5X concentration have the highest stress but the shortest elongation. The loss in mechanical qualities after 5X concentration might be attributed to nanoparticle agglomeration; also, increasing the nanoparticle concentration results decreasing in the curing process of the adhesive polymer, resulting in a drop in mechanical properties.

Flexural strength is calculated according to Eq.2 using sample dimensions and characteristics obtained from the stress-strain curves in which P is the failure force, L is the distance between pre-servers, b is the sample's width and d is the sample's thickness:

$$FlexuralStrength = \frac{3PL}{2bd^2} \tag{2}$$

The three-point flexural strength of samples with different NPs concentrations has been obtained in three replicates and is shown in Fig. 10-b. This figure shows that flexural strength of adhesive has increased by increasing the concentration of NPs. So the composites have higher mechanical properties compared to pure adhesive. The increased flexural mechanical properties have been due to a homogeneous distribution of gold NPs on the adhesive and a lack of particle agglomeration process. Adhesive dentin flexural strength has increased by 75% by increasing the concentration up to 5X gold nanoparticles. Fig. 11 shows the strengthening mecha-

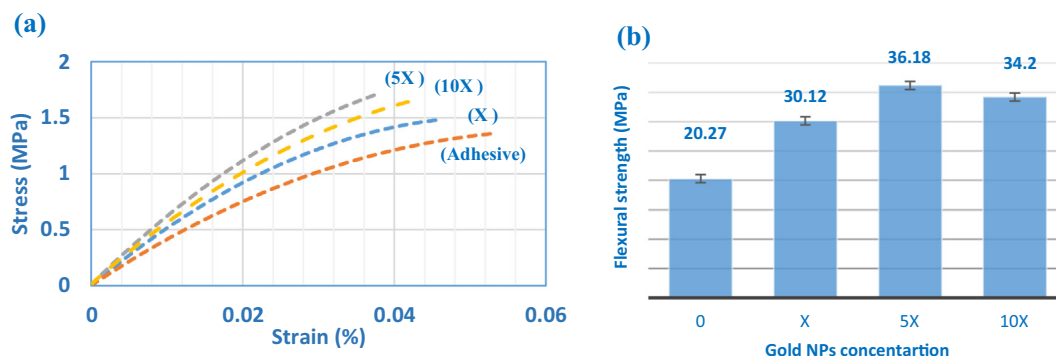


Fig. 10. stress-strain diagram of three-point flexural strength test of base adhesive sample and adhesive sample at different gold NPs concentrations, (b) the flexural strength of adhesive versus gold NPs concentration.

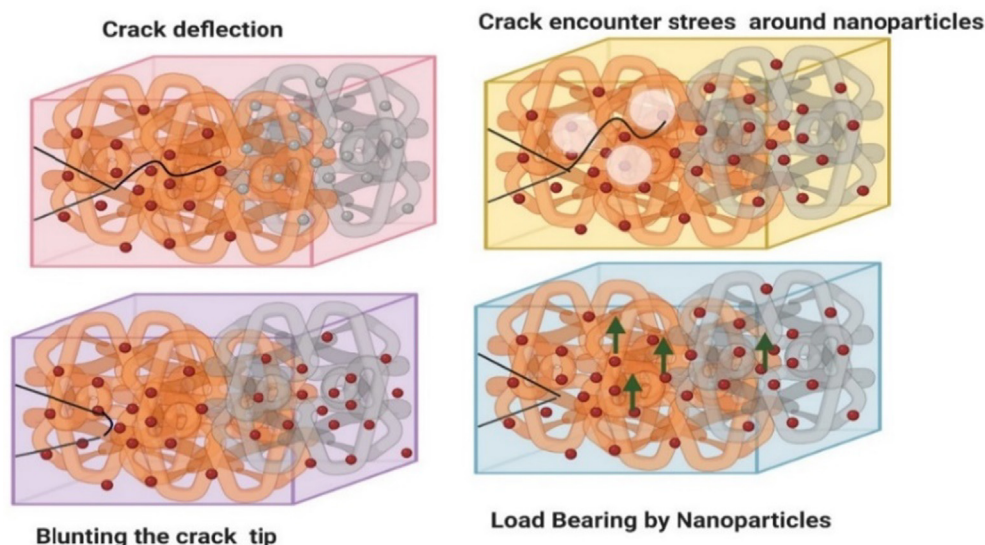
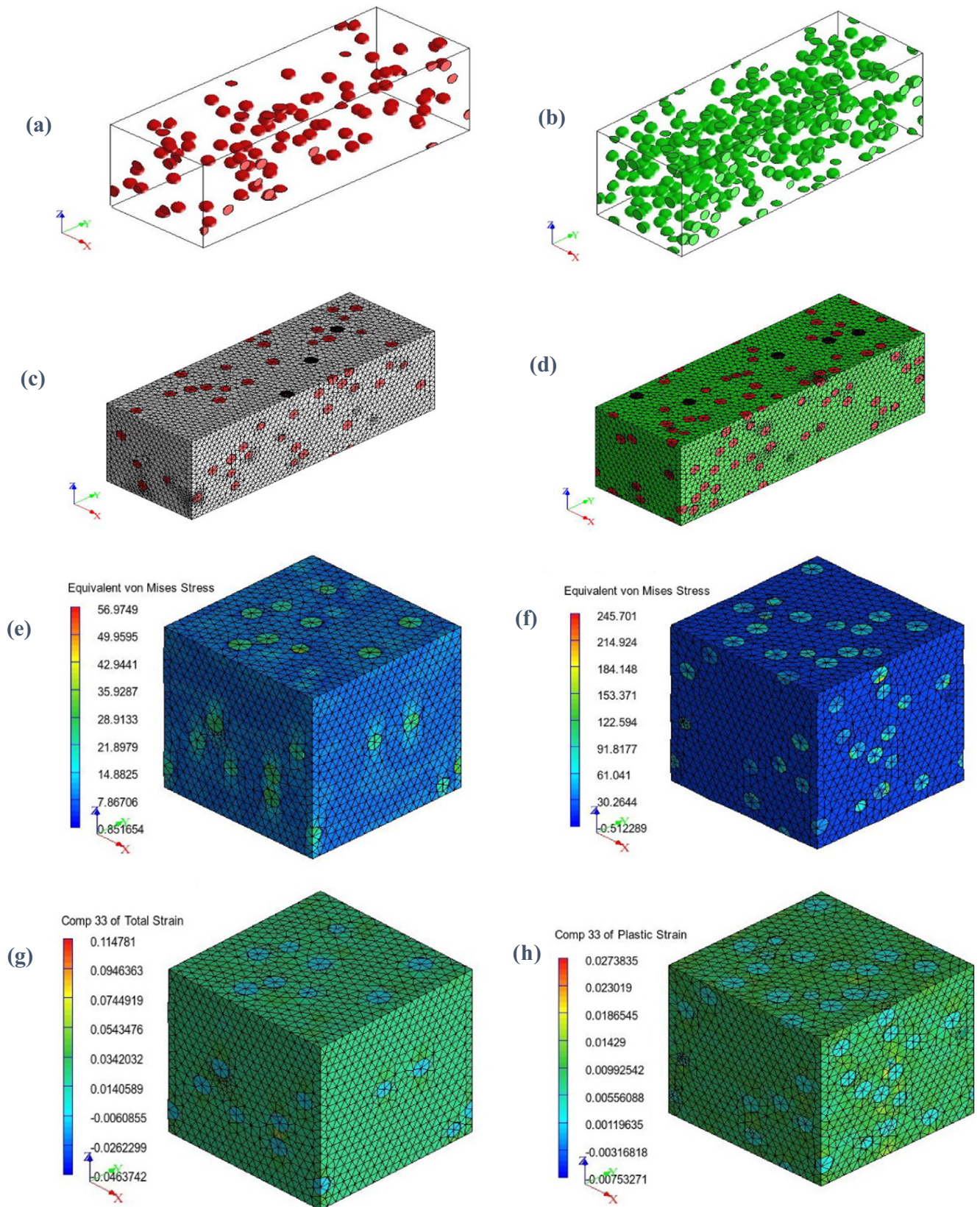


Fig. 11. schematic of mechanism of adhesive nanocomposite strengthening in presence of NPs (Created with BioRender).



**Fig.12.** (a,b) RVE model (c,d) three-dimensional mesh models (e,f) von Mises stress  $s$ , (g,h) total strain for different samples: Left 5X and right 10X.

nism of adhesive nanocomposite which includes (a) crack deflection mechanisms, (b) crack encounter stress around particles, (c) blunting the crack tip, (d) load-bearing mechanisms.

### 3.5.1. Muscale modeling of dental adhesives

In this paper, a multiscale model was used to simulate the stress and strain distribution in dental adhesives samples. The Digimat

2017.0 was applied in order to generate the appropriate micromechanical model by representing volume elements (RVE). An RVE element is considered around the matrix/reinforcement, and it is obtained under constant strain across the reinforcement and matrix. In the first step of the simulation process, a 3D geometric shape was generated while adhesive as matrix by 5x and 10X gold nanoparticles with the random phase. Fig. 12-a,b represents three-dimensional RVE shapes of the adhesive composites in which gold nanoparticles are simply assumed as circle inclusions. The design of the finite element mesh model with the quadrilateral elements

was used with the free technique and approximate size of 20 nm (Fig. 12-c,d). The von Mises stress distribution for the samples is shown in Fig. 12-e,f. The stress concentration is visible around any nanoparticles and this stress is seven times more than matrix stress for a sample having 5x nanoparticles and 5 times more for the sample with 10X nanoparticles. Also, the area of the stress concentration zone is greater where the nanoparticles are closer to each other. It demonstrates that if agglomeration occurs, a stress concentration zone will be formed, resulting in a decrease in the mechanical integrity of adhesives. Generally, the von Mises stress

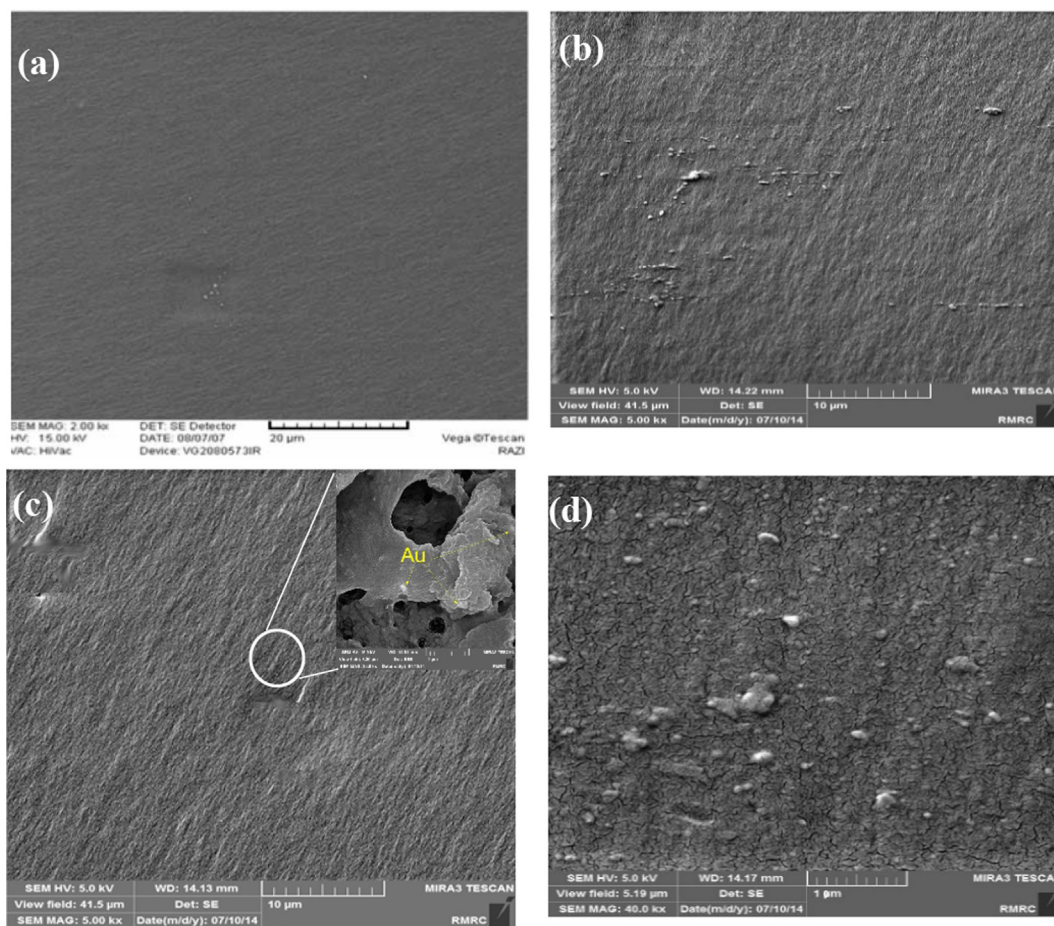


Fig. 13. SEM images of fracture surface of adhesive sample (a) without gold NPs, (b) with gold NPs concentration of 1X, (c) with gold NPs concentration of 5X (d) with gold NPs concentration of 10X.

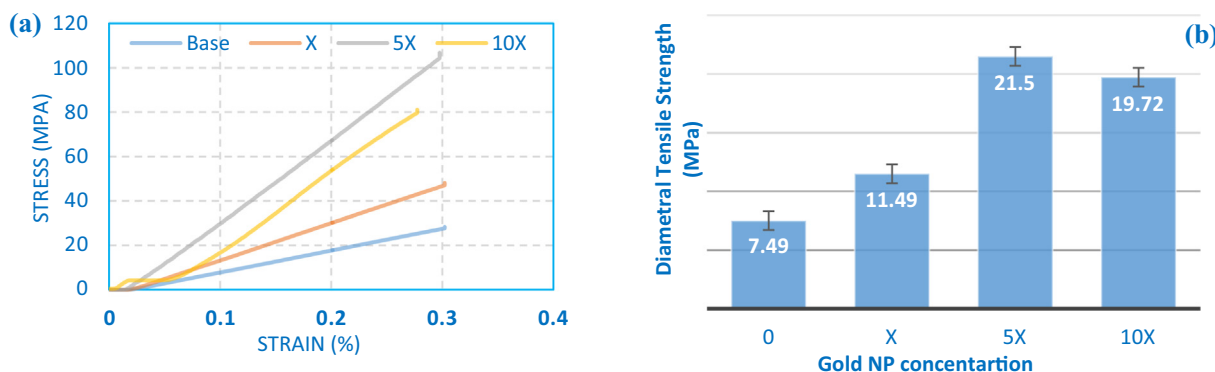


Fig. 14. (a) the stress–strain diagram of diametral tension test sample of the base adhesive sample and adhesive sample at different gold NPs concentrations, (b) variation of diametral tensile strength with NPs concentration (N = 5).

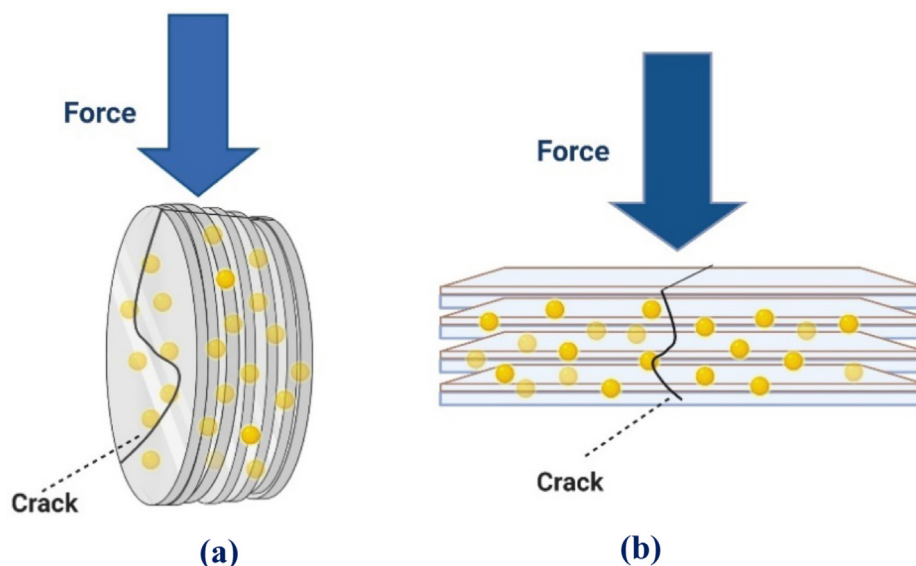


Fig. 15. schematic of effect of curing direction on crack grows of (a) diameter tensile strength, and (b) flexural strength (Created with BioRender).

for samples with 10X nanoparticles is 4–5 times greater than samples with 5X nanoparticles concentration. These results are in contrast to the graph of Fig. 10-a and this is because the agglomeration of nanoparticles was neglected in simulation process. Fig. 12-g,h shows the total strain for the samples and it can be seen that the highest strain is allocated to the polymer background and nanoparticles have strain closer to zero. Furthermore, the total strain for the sample containing 5X gold nanoparticles is six times greater than the total strain for the sample containing 10X gold nanoparticles. These findings are in excellent agreement with the experimental findings shown in Fig. 10.a. Fig. 13 shows the scanning electron micrographs of the surface fracture of sample adhesives. As shown in Fig. 13-a, the sample without gold NPs has a smooth surface which shows a completely soft fracture. Fig. 13-b,c shows the surface fracture of a sample at a concentration of X and 5X of the NPs, the brittle fracture has occurred due to the presence of NPs. There are microcracks on the surface of 10X, with higher magnification in Fig. 13-d, which shows the location of the final cracks. The presence of gold NPs has led to the slow movement of slip layers or greater adhesion to the substrate layers, which prevents the growth of cracks and ultimately enhances the strength.

### 3.5.2. Diametral tensile strength

As shown in Fig. 14-a, diametral tensile strength has been obtained using stress–strain diagrams.

Samples show a complete brittle fracture behavior. It can be seen that by increasing gold nanoparticles the stress increased. A schematic of the method of sample curing has been shown in Fig. 15. As shown in the figure, the process of layer deformation occurs in flexural strength where the force is applied perpendicular to the section of layers leading to smooth fracture. But the separation process is occurred in diametral tensile strength which will finally lead to cleavage fracture between layers [28]. This separation between layers of polymers can result in a brittle fracture of samples.

It is reasonable to predict that the three-point strength value will be greater than the diametral strength result due to the difference in fracture mode between the diametral strength and three-point strength tests, as shown in Fig. 14-a and Fig. 10-a.

The diametral tensile strength is obtained based on the sample size and the force–displacement curve through the following equation:

$$\text{DiametralTensileStrength} = \frac{2P}{\pi DL}$$

where P is a force applied at the time of fracture, D is the diameter of the sample and L is the thickness of the sample. Fig. 14-b shows the average diametral tensile strength of samples at different NPs concentrations in three replicates. The adhesive diametral tensile strength increased with increasing the concentration of gold NPs which is more significant in amount of 5X nanoparticles. As shown in the figure, reduced properties can be observed by increasing concentrations of NPs more than 5X which can be due to agglomeration of particles at higher concentrations and the creation of cracks between the interface of these agglomerates [26]. The adhesive diametral tensile strength with a concentration of 5X has had a 65% increase compared to the base adhesive.

### 3.5.3. Micro-shear bond strength (adhesion)

The effect of NPs concentration on micro-shear bond has been shown in Fig. 16. The minimum micro-shear bond of the samples is 11Mpa and the maximum amount is 18 Mpa. It can be seen that by increasing AuNPs from 5X to 10X the microshear strength decreased. According to several research, the dispersion of NPs in polymer might minimize the degree of curing the substance. Because the metallic ion reduction process may decrease the initiator or cause the polymer chains to discontinue propagating.

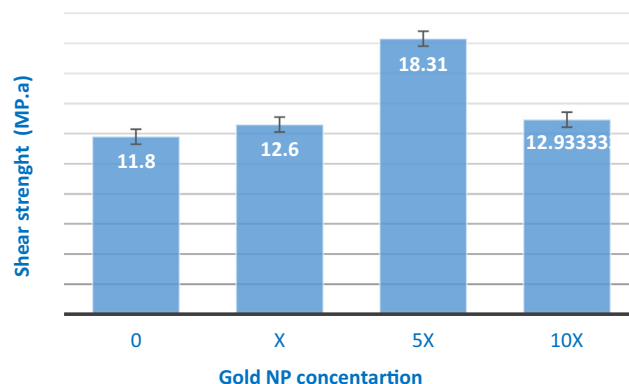
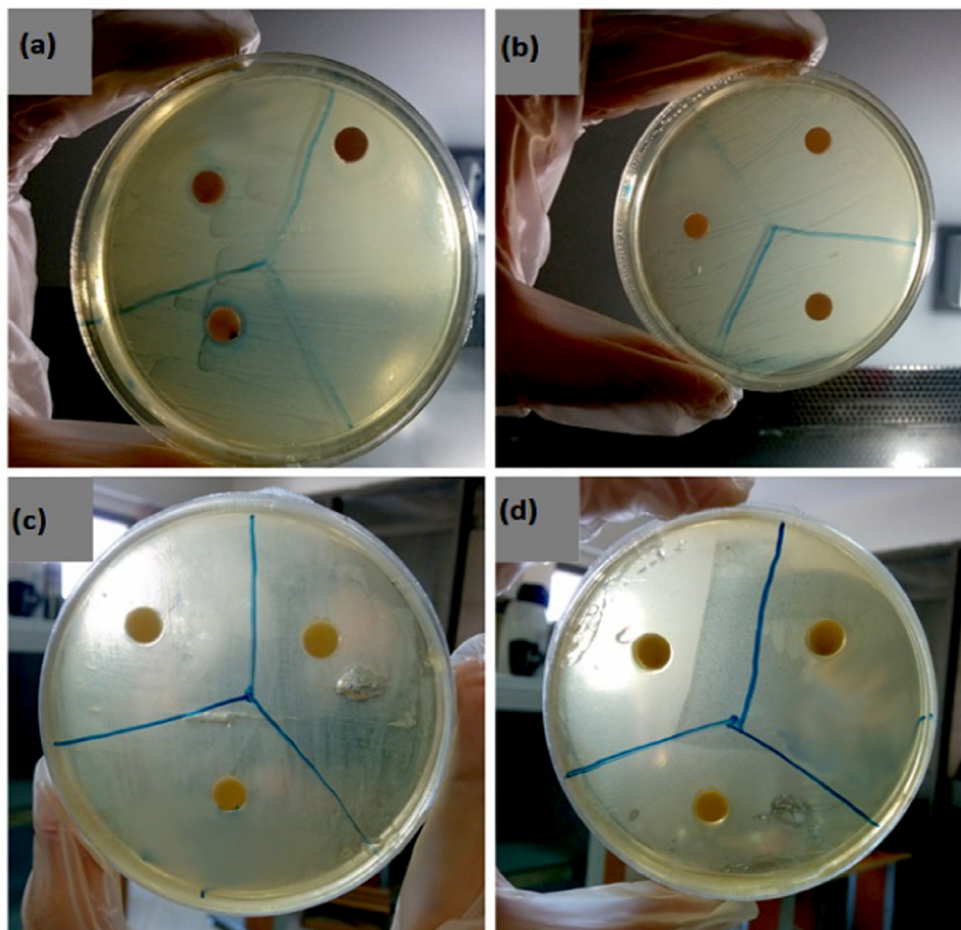


Fig. 16. The variation of micro shear strength with NPs concentration.



**Fig. 17.** the image of antibacterial results using disk diffusion method: (a) bacterial growth inhibition zone around the disc with a diameter of 2 mm at gold NPs concentration of 5X in adhesive, (b) lack of bacterial growth inhibition zone around the disc at gold NPs concentration of 10X in adhesive, (c) full growth of bacteria in the negative control, and (d) lack of bacterial growth in the positive control.

The standard deviation of samples is less than 2 except for the 10X sample, demonstrating that different samples have shown similar data in this experiment which shows the reproducibility of results. Furthermore, since micro shear samples were provided from a more significant portion of the samples, this low standard deviation demonstrates that the homogeneity of particles is excellent, resulting in the most negligible possible difference in the data acquired for all samples studied.

As mentioned earlier, the effect of NPs on adhesion can be examined through three hypotheses based on the NPs effect on (i) wettability, (ii) viscosity, and (iii) Hydrophilicity/hydrophobicity. The first two factors are dominant in lower than 5X NP concentration which enhances the adhesion, but the last factor is dominant at high NP concentrations. Furthermore, NPs used in the adhesive system in this research were hydrophilic, so adding them increases the rate of hydrophilicity and adhesion. Of course, the agglomeration plays an important role along with the first factor at higher percentages [27,28].

As shown in Fig. 16, the shear strength increases as much as 18.6 Mpa by increasing the NP at 5X concentration while significantly reduces at 10X concentration. In study conducted by Abkhezr et al. [29], the maximum adhesion rate has been obtained in 0.5 wt% of boehmite particles. The adhesion rate changes are almost similar to the adhesive system of this research. The adhe-

sion rate of commercial adhesives varies between 6 MPa and 30 M. So, the adhesion features obtained at 5X concentration are competitive with other commercial samples.

### 3.6. Antibacterial test results

#### 3.6.1. Disk diffusion method

As mentioned in the methodology section, plates placed in incubators are removed after 18 hrs and the inhibition of bacterial growth around the discs is checked. Results are summarized in

**Table 2.** The bacterial growth inhibition is well observed in the control samples, demonstrating the suitability of the test conditions.

Inhibition of bacterial growth has been observed only in the concentration of 5X in the state of pure NPs, liquid and solid adhesive. In other concentrations of gold nanoparticles inhibition was not observed.

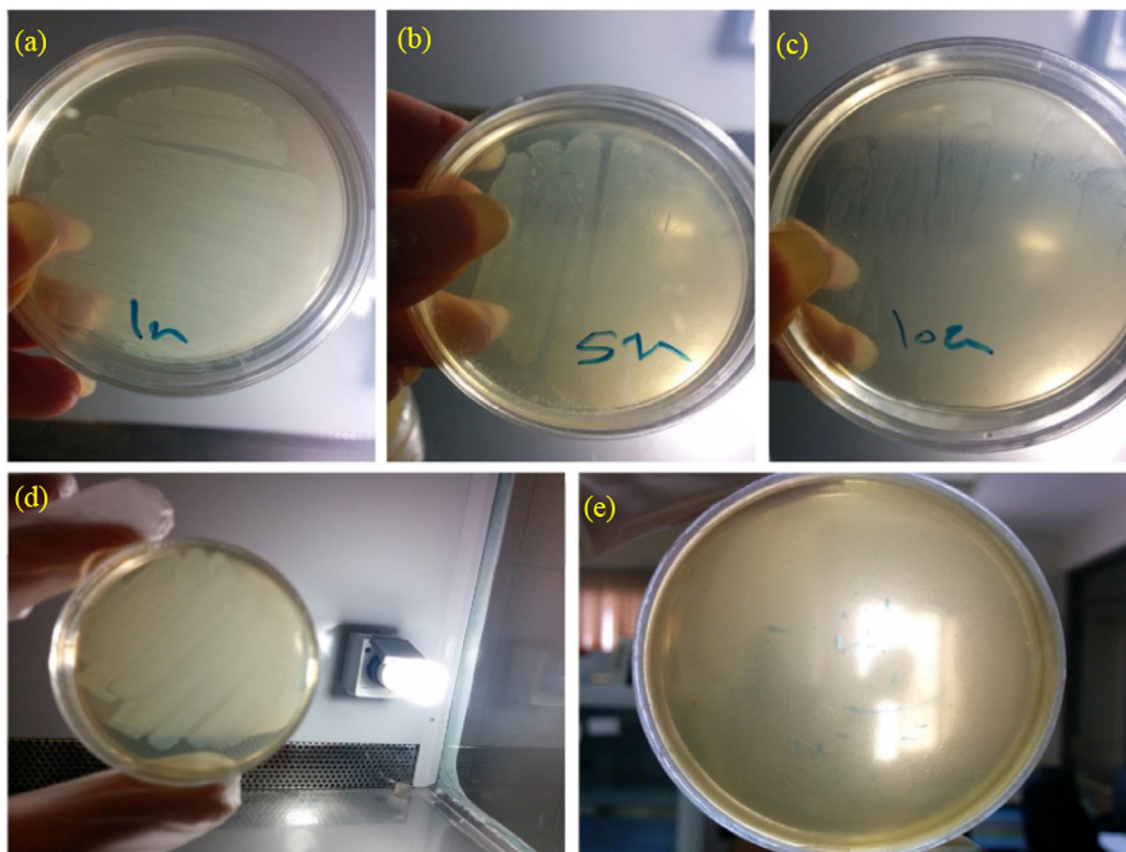
The bacterial particle diffusion process is important in all the mechanisms of actions of antibacterial NPs. At high NP concentrations, such as 10X excessive agglomeration of NPs does not allow antibacterial activity where particles aggregate and cannot penetrate the bacteria to destroy it. In other hand, NPs at lower concentrations are not at a level of being able to destroy bacteria. Fig. 17 shows the antibacterial effect images in the disk diffusion method.

**Table 2**

The summary of antibacterial test results based on disk diffusion method.

Solid dental adhesive + gold NP			Liquid dental adhesive + gold NP			gold NP (pure)		Concentration	
growth inhibition zone			growth inhibition zone			growth inhibition zone			
Repeat3	Repeat2	Repeat1	Repeat3	Repeat2	Repeat1	Repeat3	Repeat2	Repeat1	
-	-	-	-	-	-	-	-	-	X/10
-	-	-	-	-	-	-	-	-	X/5
-	-	-	-	-	-	-	-	-	1X
+	+	+	+	+	+	+	+	+	5X
-	-	-	-	-	-	-	-	-	10X
+	+	+	+	+	+	+	+	+	Control (+)
-	-	-	-	-	-	-	-	-	Control (-)

(Mark-) = inhibition was not observed = no anti-bacterial feature. (Mark +) = inhibition was observed = anti-bacterial feature.

**Fig. 18.** pour plate method test for different samples: (a) 1X gold concentration, (b) 5X gold concentration, (c) 10X gold concentration, (d) negative control, and (e) positive control.

A diameter of 2 mm of bacteria inhibition can be observed around the tablet-adhesive in the 5x sample. Thus, 5X is the optimum concentration of NPs to observe their antibacterial effect in the disk diffusion method.

### 3.6.2. Pour plate method

The pour plate experiment has been shown in Fig. 18 for the control group and sample containing antibiotics. The grows of bacteria is present in the control sample while the lack of bacterial growth is observed in the sample with an antibiotic. Positive and negative control petri dishes show bacterial growth in the absence of any antibacterial agent. The lack of bacterial growth in presence of antibiotics proves the accuracy of antibacterial test conditions. As shown in Fig. 18, the complete bacterial growth inhibition was observed in the pour plate method. The bacterial growth rate

has decreased by increasing the concentration of NPs from 1X to 10X. So by increasing the gold NPs concentration, their effectiveness in killing bacteria increases [30]. This test demonstrated the functional adhesive's superior antibacterial properties. A considerable number of nanosized (20 nm) nanospheres were seen on the surface of samples after the AuNPs were loaded. It was shown that they were uniformly dispersed with no visible agglomeration on the surface of the sample confirmed by EDAX analysis. Gram-positive and gram-negative bacteria have both been shown to be susceptible to AuNPs. The mechanism behind AuNPs' antibacterial activities has been suggested to be strongly connected to Au ions. AuNPs have the capacity to interact with bacterial cell membranes, increasing permeability and disrupting respiration. Also, Au ion penetration may cause adenosine triphosphate (ATP) generation and DNA replication to be disrupted. In addition, AuNPs and Au

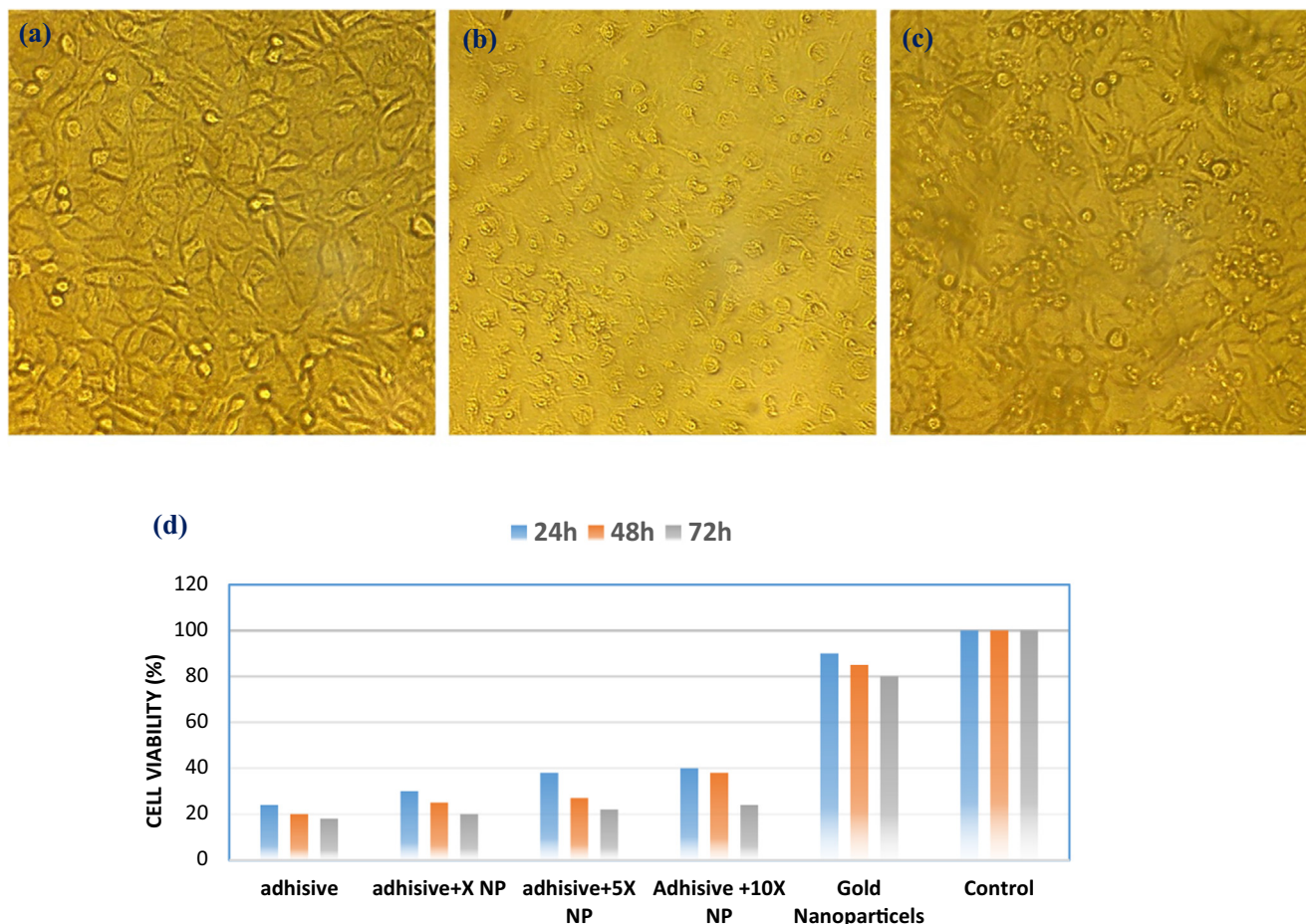


**Fig. 19.** optical microscopy images showing cellular morphologies of L929 cells after treatment for 72 hrs for (a) control cell, (b) cell + adhesive nanocomposites, (c) gold NPs, (d) cell viability graph of L929 cells treated with gold NPs and adhesive.

ions may increase the generation of reactive oxygen species (ROS), which can damage cell membranes, mitochondria, and DNA by attacking membrane lipids.

### 3.7. MTT assay

In Fig. 19-a,b,c shows the optical microscopy images of L929 fibroblast cells exposed to adhesive and gold NPs. Gold NPs and base adhesive induced cellular morphology change in L929 cells. Cytotoxicity evaluation of gold NPs incorporated adhesives was done using MTT assay. Cells in their exponential growth phase with a density of 7000 cells/well were seeded in a 96-well plate and were incubated for 12 hrs at 37 °C in a 5% CO<sub>2</sub> incubator. Untreated cells, as well as the cell treated with different concentrations of gold NPs, were subjected to the MTT assay for cell viability determination. Cytotoxicity was assessed at different periods (24, 48, and 72 hrs.) at different gold NPs concentrations. The incorporation of gold NPs increased the cell viability of base adhesive. The cell viability of samples after 24hs of incubation was slightly higher than the same samples after 72 hrs of incubation (Fig. 19-d).

## 4. Conclusions

XRD, SEM, and UV-Vis spectrophotometry have been carried out to study the particle size and purity of the gold NPs. The results show that the incorporation of 20 nm gold NPs in the adhesive composition is successfully done. It has also been determined that NPs significantly increase the mechanical properties of adhesive.

Furthermore, most of the samples related to disk methods show bacterial growth but only the presence of NP at concentration of 5X shows a reduced rate of bacterial growth. So, the concentration of 5X is the optimum concentration to activate the anti-bacterial feature of dental adhesives. Moreover, the cytotoxicity study results show that the toxicity of dental adhesive containing gold NPs is higher than the pure gold NPs but still less than the pure base adhesive without gold NPs.

### Data availability

Data will be made available on request.

### Declaration of Competing Interest

The authors declare that they have no known competing financial interests or personal relationships that could have appeared to influence the work reported in this paper.

### Acknowledgment

The authors would like to acknowledge technical support and valuable assistance of the Institutes for NanoBiomedical Research, Rutgers University. We are especially grateful to anonymous reviewers for their valuable and constructive comments.

## Appendix A. Supplementary material

Supplementary data to this article can be found online at <https://doi.org/10.1016/j.molliq.2022.119824>.

## References

- [1] E. Sofan et al., Classification review of dental adhesive systems: from the IV generation to the universal type, *Annali di stomatologia* 8 (1) (2017) 1–17.
- [2] W. Zhou, S. Liu, X. Zhou, M. Hannig, S. Rupf, J. Feng, X. Peng, L. Cheng, Modifying adhesive materials to improve the longevity of resinous restorations, *Int. J. Mol. Sci.* 20 (3) (2019) 723.
- [3] Powers, J.M. and R.L. Sakaguchi, *Craig's restorative dental materials*, 13/e. 2006: Elsevier India.
- [4] K. Subramani et al., Biofilm on dental implants: a review of the literature, *Int. J. Oral Maxillofac. Implants* 24 (4) (2009).
- [5] B. Pratap, R.K. Gupta, B. Bhardwaj, M. Nag, Resin based restorative dental materials: characteristics and future perspectives, *Japanese Dental Science Review* 55 (1) (2019) 126–138.
- [6] E. Senses, C.L. Kitchens, A. Faraone, Viscosity reduction in polymer nanocomposites: Insights from dynamic neutron and X-ray scattering, *Journal of Polymer Science* 60 (7) (2022) 1130–1150.
- [7] R.J. Turner, Metal-based antimicrobial strategies, *Microb. Biotechnol.* 10 (5) (2017) 1062–1065.
- [8] W. Salem, D.R. Leitner, F.G. Zingl, G. Schratler, R. Prassl, W. Goessler, J. Reidl, S. Schild, Antibacterial activity of silver and zinc nanoparticles against *Vibrio cholerae* and enterotoxic *Escherichia coli*, *Int. J. Med. Microbiol.* 305 (1) (2015) 85–95.
- [9] K. Yorseng, S. Siengchin, B. Ashok, A.V. Rajulu, Nanocomposite egg shell powder with in situ generated silver nanoparticles using inherent collagen as reducing agent, *Journal of Bioresources and Bioproducts* 5 (2) (2020) 101–107.
- [10] B. Ashok, N. Hariram, S. Siengchin, A.V. Rajulu, Modification of tamarind fruit shell powder with in situ generated copper nanoparticles by single step hydrothermal method, *J. Bioresources Bioproducts* 5 (3) (2020) 180–185.
- [11] K. Punjabi, S. Mehta, R. Chavan, V. Chitalia, D. Deogharkar, S. Deshpande, Efficiency of biosynthesized silver and zinc nanoparticles against multi-drug resistant pathogens, *Front. Microbiol.* 9 (2018).
- [12] M. Shimabukuro, Antibacterial property and biocompatibility of silver, copper, and zinc in titanium dioxide layers incorporated by one-step micro-arc oxidation, *A Review. Antibiotics* 9 (10) (2020) 716.
- [13] K.S. Siddiqi, A. ur Rahman, Tajuddin, A. Husen, Properties of zinc oxide nanoparticles and their activity against microbes, *Nanoscale Res. Lett.* 13 (1) (2018).
- [14] S. Kasraei, L. Sami, S. Hendi, M.-Y. AliKhani, L. Rezaei-Soufi, Z. Khamverdi, Antibacterial properties of composite resins incorporating silver and zinc oxide nanoparticles on *Streptococcus mutans* and *Lactobacillus*, *Restor Dent Endod* 39 (2) (2014) 109.
- [15] H. Jia, W. Hou, L. Wei, B. Xu, X. Liu, The structures and antibacterial properties of nano-SiO<sub>2</sub> supported silver/zinc–silver materials, *Dent. Mater.* 24 (2) (2008) 244–249.
- [16] S. Sadhasivam, P. Shanmugam, K. Yun, Biosynthesis of silver nanoparticles by *Streptomyces hygroscopicus* and antimicrobial activity against medically important pathogenic microorganisms, *Colloids Surf., B* 81 (1) (2010) 358–362.
- [17] Allaker, R.P., The Use of Antimicrobial Nanoparticles to Control Oral Infections, in *Nano-Antimicrobials: Progress and Prospects*, N. Cioffi and M. Rai, Editors. 2012, Springer Berlin Heidelberg: Berlin, Heidelberg. p. 395–425.
- [18] K.M. Reddy, K. Feris, J. Bell, D.G. Wingett, C. Hanley, A. Punnoose, Selective toxicity of zinc oxide nanoparticles to prokaryotic and eukaryotic systems, *Appl. Phys. Lett.* 90 (21) (2007).
- [19] Ravishankar Rai, V. and A. Jamuna Bai, Nanoparticles and their potential application as antimicrobials. *Science Against Microbial Pathogens: Communicating Current Research and Technological Advances*, Mendez-Vilas, A.(Ed.). University of Mysore, India, 2011: p. 197–209.
- [20] K. Umamaheswari, R. Baskar, K. Chandru, N. Rajendiran, S. Chandirasekar, Antibacterial activity of gold nanoparticles and their toxicity assessment, *BMC Infect. Dis.* 14 (S3) (2014).
- [21] S. Priyadarsini, S. Mukherjee, M. Mishra, Nanoparticles used in dentistry: a review, *J. Oral Biol. Craniofacial Res.* 8 (1) (2018) 58–67.
- [22] R. Ramachandran, C. Krishnaraj, V.K.A. Kumar, S.L. Harper, T.P. Kalaiichelvan, S.-I. Yun, In vivo toxicity evaluation of biologically synthesized silver nanoparticles and gold nanoparticles on adult zebrafish: a comparative study, *Biotech* 8 (10) (2018).
- [23] C. Su et al., Antibacterial properties of functionalized gold nanoparticles and their application in oral biology, *J. Nanomater.* 2020 (2020) 5616379.
- [24] Y. Cui, Y. Zhao, Y. Tian, W. Zhang, X. Lü, X. Jiang, The molecular mechanism of action of bactericidal gold nanoparticles on *Escherichia coli*, *Biomaterials* 33 (7) (2012) 2327–2333.
- [25] Z. Ebadi, M. Atai, M. Ebrahimi, Mechanical and anti-bacterial properties of dental adhesive containing diamond nanoparticles, *Science and Technology* 24 (2) (2011) 121–131.
- [26] M. Miyazaki, S. Ando, K.o. Hinoura, H. Onose, B.K. Moore, Influence of filler addition to bonding agents on shear bond strength to bovine dentin, *Dent. Mater.* 11 (4) (1995) 234–238.
- [27] G.J. Eckert, J.A. Platt, A statistical evaluation of microtensile bond strength methodology for dental adhesives, *Dent. Mater.* 23 (3) (2007) 385–391.
- [28] J.-S. Kim, B.-H. Cho, I.-B. Lee, C.-M. Um, B.-S. Lim, M.-H. Oh, C.-G. Chang, H.-H. Son, Effect of the hydrophilic nanofiller loading on the mechanical properties and the microtensile bond strength of an ethanol-based one-bottle dentin adhesive, *J. Biomed. Mater. Res. B Appl. Biomater.* 72B (2) (2005) 284–291.
- [29] A. Abkhezr et al., Properties of dental adhesives incorporated with boehmite nano-particles, *Iran. J. Polym. Sci. Technol. (In Persian)* 23 (2011) 423–433.
- [30] H. Gu, P.L. Ho, E. Tong, L. Wang, B. Xu, Presenting vancomycin on nanoparticles to enhance antimicrobial activities, *Nano Lett.* 3 (9) (2003) 1261–1263.
- [31] R. Xiong et al., Photothermal nanofibres enable safe engineering of therapeutic cell, *Nat. Nanotechnol.* 16 (2021) 1281–1291.
- [32] A. Kamyar, M. Khakbiz, A. Zamanian, M. Yasaei, B. Yarmand, Synthesis of a novel dexamethasone intercalated layered double hydroxide nanohybrids and their deposition on anodized titanium nanotubes for drug delivery purposes, *J. Solid State Chem.* 271 (2019) 144–153.
- [33] M. Yasaei, M. Khakbiz, A. Zamanian, E. Ghasemi, Synthesis, and characterization of Zn/Al-LDH@SiO<sub>2</sub> nanohybrid: intercalation and release behavior of vitamin C, *Mater. Sci. Eng., C* 103 (2019) 109816.